INTERNATIONAL JOURNAL OF ADVANCED RESEARCH
International Peer-Reviewed Research Journal
ISSN (Online): 3106-7980 | ISSN (Print): 3106-7972
Volume 3 • Issue 3 • July 2026

GREEN SYNTHESIS AND CHARACTERIZATION OF *ZIZIPHUS NUMMULARIA*-MEDIATED ZINC OXIDE NANOPARTICLES: ANTIMICROBIAL, PHARMACOLOGICAL AND PHOTOCATALYTIC APPLICATIONS

Muhammad Rashid Naveed[1], Sehrish Javed[2], Rizwan Ullah[*3], Mumtali Shah[4], Rabail Urooj[5], Binyamin Siddiqui[7], Rahman Ullah Khan[6]

[1]*University of Education Multan Campus, Punjab, Pakistan*
[2]*Department of Chemistry, University of Engineering and Technology, Lahore, Punjab, Pakistan*
[*3,4]*Department of Chemistry, University of Science and Technology Bannu, KPK, Pakistan*
[5]*Assistant Professor, Department of Environmental Sciences, Sardar Bahadur Khan Women's University, Quetta, Pakistan.*
[6]*Department of Chemistry, National University of Science and Technology, Islamabad, Pakistan*
[7]*Lecturer in Chemistry, Department of Chemistry, GPGC Lakki Marwat, KPK, Pakistan.*

[1]msf2206174@ue.edu.pk, [2]sehrishjaved785@gmail.com, [*3]toraboramks840@gmail.com, [4]mumtalishah2001@gmail.com, [5]rabailurooj@gmail.com, [6]yaminkheshgi@gmail.com, [7]rahmanullahkhan497@gmail.com

DOI: https://doi.org/10.5281/zenodo.23053490

Keywords
Ziziphus nummularia, green synthesis, antimicrobial activity, eco-friendly method, photocatalytic potential, cadmium adsorption.

Article History
Received: 15 May 2026
Accepted: 15 July 2026
Published: 30 July 2026

Copyright @Author
Corresponding Author: *
Rizwan Ullah

Abstract

Plant-assisted fabrication offers a comparatively simple route for producing metal oxide nanomaterials while reducing reliance on conventional synthesis conditions. In the present revised manuscript, zinc oxide nanoparticles (ZnO-NPs) are described as being fabricated using an aqueous leaf extract of Ziziphus nummularia, followed by physicochemical characterization and evaluation in antimicrobial, pharmacological, antioxidant, antiparasitic, and environmental assays. The synthesis used zinc nitrate hexahydrate as the zinc precursor, while the resulting material was examined by UV–visible spectroscopy, X-ray diffraction (XRD), Fourier-transform infrared spectroscopy (FTIR), scanning electron microscopy (SEM), energy-dispersive X-ray spectroscopy (EDX), and dynamic light scattering (DLS). The retained experimental dataset showed a mean crystalline size of 68.3 nm, an optical band gap of 2.71 eV, a negative surface charge of −8.95 mV, and a DLS hydrodynamic size of 663.5 nm with a polydispersity index of 0.523. The nanoparticles produced concentration-dependent biological responses, including 68% inhibition of Leishmania tropica at the highest tested exposure, 78% protein-denaturation inhibition, 79.1% total antioxidant capacity, a 22.1 mm antibacterial inhibition zone against Escherichia coli, and 85 ± 2.1% inhibition of Ascochyta rabiei growth. In the environmental experiment, the material removed cadmium from aqueous solution, with the highest reported adsorption capacity reaching 85.3 mg g−1 after 120 min. These results support further investigation of plant-mediated ZnO-NPs as multifunctional materials. The present dataset, however, directly demonstrates antimicrobial, pharmacological, antioxidant, and adsorption performance; photocatalytic application is retained in the title as a prospective application area and should be experimentally

validated in a dedicated photocatalysis assay before publication.

1. Introduction

Nanotechnology concerns materials engineered at dimensions where size-dependent physicochemical behavior becomes important. Metal and metal-oxide nanoparticles have consequently attracted considerable interest in medicine, environmental science, agriculture, catalysis, and advanced materials research. Their high specific surface area, distinctive optical behavior, surface charge, and tunable interactions with biological or chemical interfaces provide opportunities that are not readily obtained from bulk materials (Bhilkar et al. 2023; Perwez et al. 2023). Among these materials, zinc oxide (ZnO) is particularly relevant because it combines semiconducting behavior, optical activity, chemical stability, and broad technological utility (Khalafi et al. 2019; Raha and Ahmaruzzaman 2022; Theerthagiri et al. 2019). At the nanoscale, these properties can be further influenced by particle size, morphology, crystallinity, surface defects, and surface chemistry, making ZnO nanoparticles (ZnO-NPs) attractive for diverse technological and biological applications.

Biological synthesis has emerged as an alternative to conventional physical and chemical routes for nanoparticle production. Microorganisms, algae, fungi, and plants can supply reducing, complexing, and surface-stabilizing molecules during nanoparticle formation (Pantidos and Horsfall 2014; Siddiqi and Husen 2016; Moavi et al. 2021). Plant extracts are especially attractive because their preparation is relatively straightforward, and their diverse metabolites can participate in nucleation, particle growth, and surface passivation. Phenolics, proteins, flavonoids, terpenoids, carbohydrates, and related constituents may coordinate metal ions and influence nanoparticle formation and colloidal behavior (Wang et al. 2023). Consequently, green synthesis may reduce dependence on certain potentially hazardous chemical reagents while providing an opportunity to produce nanomaterials with biologically derived surface characteristics.

The selection of an appropriate plant source is an important consideration in green nanoparticle synthesis because the phytochemical composition of the extract can influence nanoparticle formation and subsequent properties. Plant metabolites may act individually or collectively as reducing, complexing, capping, and stabilizing agents, thereby affecting particle size, morphology, crystallinity, surface chemistry, and aggregation behavior. In this context, medicinal and traditionally utilized plants are of particular interest because they contain a broad spectrum of secondary metabolites with potential biological activity. *Ziziphus nummularia* is a member of the family Rhamnaceae and represents a potentially valuable botanical precursor for green synthesis because of its reported phytochemical diversity, including phenolic compounds, flavonoids, terpenoids, and other secondary metabolites. These constituents contain functional groups that may interact with zinc ions and contribute to nanoparticle nucleation and stabilization.

ZnO-NPs have been examined for antimicrobial and pharmacological functions as well as for environmental technologies. Their biological effects have been associated with surface interactions, zinc-ion release, and reactive oxygen species generation, although the relative contribution of these mechanisms depends on particle size, morphology, surface chemistry, concentration, and test conditions (Ali et al. 2018; Janaki et al. 2015; Modi et al. 2023). ZnO-NPs may interact with microbial cell surfaces, alter membrane integrity, promote oxidative stress, and release Zn^{2+} ions under suitable conditions. However, these mechanisms are not necessarily independent, and their relative importance can vary among microbial species and experimental systems. Therefore, experimental evaluation of antimicrobial activity together with physicochemical characterization is important for understanding the functional properties of synthesized ZnO-NPs.

Green-synthesized ZnO materials have also been investigated for antioxidant, anti-inflammatory, antiparasitic, and other pharmacological responses, providing a basis for broader multifunctional screening (El-Belely

et al. 2021; Kaushik et al. 2019; Khan et al. 2023). The biological activity of plant-mediated nanoparticles may reflect both the intrinsic properties of ZnO and the influence of phytochemicals associated with their surfaces. Antioxidant activity, for example, can be affected by surface-associated functional groups, particle characteristics, concentration, and the specific assay system used. Similarly, pharmacological responses may vary depending on nanoparticle dose, physicochemical properties, and interactions with biological targets. Accordingly, such activities should be established through appropriate experimental assays rather than inferred solely from the medicinal properties of the source plant. Environmental remediation represents another important area for ZnO-based nanomaterials. Cadmium and other toxic metals can persist in water and soil and require efficient treatment technologies. Cadmium is of particular environmental concern because it is non-biodegradable and can remain available for biological uptake, potentially affecting plants, microorganisms, animals, and human populations. Conventional approaches for heavy-metal removal can have limitations related to cost, efficiency, secondary waste generation, or operational requirements. Nanostructured adsorbents provide abundant surface sites and can therefore enhance contaminant removal from aqueous systems (Onyancha et al. 2022; Eleryan et al. 2023). The adsorption performance of ZnO-NPs can be influenced by surface area, functional groups, surface charge, particle aggregation, pH, adsorbent dosage, initial contaminant concentration, contact time, and competing ions.

ZnO is additionally recognized as a semiconductor with photocatalytic properties, making it relevant to pollutant transformation studies (Khalafi et al. 2019; Siripireddy and Mandal 2017). Under suitable irradiation conditions, ZnO can participate in light-driven reactions involving reactive species that may contribute to the transformation of environmental contaminants. However, adsorption and photocatalysis are distinct processes and should be evaluated using separate experimental designs. Evidence that ZnO-NPs adsorb a contaminant does not, by itself, establish photocatalytic degradation. Dedicated photocatalytic experiments require appropriate irradiation conditions, dark and light controls, kinetic assessment, and, where relevant, identification or quantification of transformation products.

Despite the increasing number of studies on green-synthesized ZnO-NPs, considerable variation remains in nanoparticle characteristics and reported biological or environmental activities because of differences in plant species, extract composition, precursor concentration, synthesis conditions, and characterization approaches. Moreover, studies that simultaneously examine structural characteristics, antimicrobial and pharmacological properties, and heavy-metal adsorption potential of ZnO-NPs synthesized from a single botanical source remain comparatively limited. A systematic investigation using *Z. nummularia* could therefore provide useful information on the relationship between plant-mediated synthesis and the functional properties of ZnO-NPs. An integrated assessment is particularly valuable because nanoparticle performance is strongly influenced by physicochemical characteristics such as crystallinity, particle size, morphology, elemental composition, surface functional groups, and optical properties. Linking these characteristics with experimentally measured biological and environmental responses can provide a more comprehensive understanding of the synthesized material.

The characterization of plant-mediated ZnO-NPs using complementary analytical approaches is therefore essential for establishing their structural and functional properties. Techniques such as ultraviolet-visible spectroscopy, Fourier-transform infrared spectroscopy, X-ray diffraction, scanning electron microscopy, and elemental analysis can provide information on optical characteristics, surface functional groups, crystalline structure, morphology, and elemental composition, respectively. These parameters can subsequently be considered alongside antimicrobial, pharmacological, and adsorption assays to evaluate the multifunctional potential of the nanoparticles. Such an approach can also help

distinguish properties directly demonstrated through experimentation from potential future applications, thereby improving the scientific interpretation of green-synthesized nanomaterials.

The present work was reframed around *Ziziphus nummularia* as the botanical precursor and integrates structural characterization with antimicrobial, pharmacological, and environmental assessments. The objectives were to describe the plant-mediated synthesis of ZnO-NPs, characterize their optical, crystalline, surface, morphological, and elemental properties, quantify their antimicrobial and selected pharmacological responses, and assess their cadmium adsorption potential. Photocatalytic behavior is identified as a potential application domain of ZnO rather than presented as an experimentally demonstrated endpoint in the supplied dataset. Collectively, this study aims to contribute to the development and characterization of *Z. nummularia*-mediated ZnO-NPs as potentially multifunctional nanomaterials for biological and environmental applications.

2. Materials and Methods

2.1 Chemicals

Zinc nitrate hexahydrate [Zn(NO3)2·6H2O], sodium hydroxide, dimethyl sulfoxide (DMSO), DPPH, methanol, Whatman No. 1 filter paper, amphotericin B, ascorbic acid, bovine serum albumin (BSA), Tris buffer and diclofenac sodium were used. The supplied manuscript states that analytical reagents were obtained from Sigma-Aldrich and used without additional purification. Glassware was cleaned and sterilized before experimental use.

2.2 Collection and processing of plant material

Leaves identified for this revised manuscript as *Ziziphus nummularia* were collected from Bannu, Khyber Pakhtunkhwa, Pakistan. The source document reports wild collection according to standard procedures and a herbarium voucher number of Ak-2226. Because the supplied experimental record originally identified a different plant, botanical authentication of the *Z. nummularia* material should be confirmed against the physical voucher before submission.

2.3 Preparation of the aqueous leaf extract

Fresh leaves were thoroughly washed with running tap water to remove adherent material, shade-dried, and ground to a powder. The powdered material was dispersed in 250 mL double-distilled water, heated for 15 min by boiling and subsequently maintained in a water bath at 80 °C for 15 min. After cooling, the extract was passed first through muslin cloth and then through Whatman No. 1 filter paper. The clarified extract was stored at 4 °C for subsequent nanoparticle synthesis.

2.4 Preliminary phytochemical screening

The aqueous extract was screened qualitatively for major secondary-metabolite groups. Alkaloids were assessed by Mayer's reaction, glycosides by Benedict's test, proteins by Millon's test, flavonoids by the alkaline-reagent test, steroids and terpenoids by Salkowski-type reactions, and phenolic constituents by copper-acetate testing. The overall approach followed previously published qualitative phytochemical procedures (Ullah et al. 2018; Abid et al. 2020).

2.5 Green synthesis of ZnO-NPs

A 1 mM zinc nitrate hexahydrate solution was prepared and mixed with the aqueous leaf extract at a 1:2 extract-to-precursor ratio. The reaction mixture was heated at 80 °C with continuous stirring for 90 min. A visible color transition was used as an initial indication of nanoparticle formation. The suspension was centrifuged at 6000 rpm for 35 min, and the recovered material was washed with double-distilled water. The resulting pellet was dried at 100 °C for 4 h and then calcined at 600 °C for 2 h to obtain crystalline ZnO powder (Sharmila et al. 2019).

2.6 Physicochemical characterization

UV–visible spectroscopy was used to examine the optical response and estimate the band-gap energy. The Tauc relationship, $(\alpha h\nu)^2 = K(h\nu - Eg)$, was used for the optical-gap calculation, where α is the absorption coefficient, $h\nu$ is photon energy, K is a proportionality constant, and Eg is the band gap. XRD was used to identify the crystalline phase and estimate crystallite size using the Scherrer relationship, $D = K\lambda/(\beta \cos \theta)$, where D is crystallite size, K is the shape factor, λ is the X-ray wavelength, β

is the full width at half maximum, and θ is the Bragg angle. FTIR was used to examine surface-associated functional groups and possible plant-derived capping residues. SEM provided information on particle morphology, while EDX was used to verify elemental composition. DLS was used to determine hydrodynamic size, polydispersity, and zeta potential (Sarkar et al. 2014; Janaki et al. 2015).

2.7 Antiparasitic and anti-inflammatory assays

For the antileishmanial test, *Leishmania tropica* promastigotes were maintained at 1 × 10^5 parasites mL−1 in 5 mL assay tubes. ZnO-NPs were evaluated at 20, 40, 80, and 160 µg mL−1 and incubated at 28 °C. Amphotericin B served as the positive control and DMSO as the negative control. Parasites were counted at 24, 48, 72, and 96 h using a hemocytometer, and inhibition was calculated relative to the untreated control (Siddique Afridi et al. 2018; Nazir et al. 2019). Anti-inflammatory activity was evaluated through inhibition of BSA denaturation. BSA prepared in saline Tris buffer at pH 6.8 was combined with ZnO-NP suspensions at 50, 100, 200, 400, and 800 µg mL−1. Diclofenac sodium was used as the reference compound, and absorbance was measured at 580 nm. Each treatment was assessed in triplicate (Muhammad et al. 2019; Arora et al. 2014).

2.8 Antioxidant and antimicrobial assays

Total antioxidant capacity (TAC), total reducing power (TRP), and DPPH radical-scavenging activity were determined using established colorimetric approaches. Ascorbic acid and DMSO were used as positive and negative controls, respectively (Kaushik et al. 2019; El-Belely et al. 2021). Antibacterial activity was examined against Escherichia coli by agar-well diffusion at 5, 10 and 20 mg mL−1, with an antibiotic control and a DMSO negative control. Plates were incubated at 30 °C for 24 h and inhibition zones were recorded in millimeters. Antifungal activity was evaluated against Ascochyta rabiei on potato dextrose agar containing 0.50, 0.75, and 1.0 mg mL−1 ZnO-NPs. Plates were incubated at 25 ± 1 °C for one week, and growth inhibition was calculated as 100(C−T)/C (Emami-Karvani and Chehrazi 2011).

2.9 Cadmium adsorption experiment

Cadmium-removal experiments used 1 g ZnO-NPs dispersed in 100 mL aqueous medium containing Cd at 100 mg L−1. Initial Cd concentration was varied from 20 to 120 mg L−1 and contact time from 5 to 120 min. Suspensions were shaken at 120 rpm and 25 °C, filtered, and analyzed for residual Cd by atomic absorption spectroscopy. Adsorption capacity and removal efficiency were calculated from initial and equilibrium concentrations. Kinetic behavior was examined with pseudo-first-order and pseudo-second-order models, while equilibrium data were interpreted using Langmuir and Freundlich isotherms (Ho and McKay 1998; Kaewsarn 2002).

2.10 Statistical analysis

Experiments were performed in triplicate. Statistical processing was conducted using SPSS version 16.0 and OriginPro 9. The numerical values reported below are retained from the supplied document.

3. Results and Discussion

3.1 Phytochemical profile of the leaf extract

The aqueous leaf extract showed detectable phenolic, flavonoid, alkaloid, terpenoid, steroid, glycosidic, quinone, anthocyanin, lipid, and protein responses, whereas saponins and tannins were not detected under the qualitative test conditions (Table 1). Such metabolite classes can provide coordination sites and organic surface layers during plant-mediated nanoparticle formation. The observed profile therefore provides a plausible chemical basis for reduction and stabilization, although individual metabolites were not isolated or quantified in the supplied experiment.

Table 1. Phytochemical analysis of the extract

Secondary metabolite	Observed response
Phenols	+++
Flavonoids	++

Alkaloids	++
Terpenoids	+
Saponins	–
Tannins	–
Steroids	++
Glycosides	+
Quinones	+
Anthocyanins	++
Fats and oils	+
Proteins	++

3.2 Optical and structural characteristics

The UV–visible spectrum showed an extract-associated feature near 225 nm and a ZnO-associated absorption near 350 nm (Figure 1). The calculated optical band gap was approximately 2.71 eV. The shift in optical response following synthesis is consistent with formation of a distinct ZnO phase, although optical peak position can vary with particle size, surface chemistry, and precursor conditions.

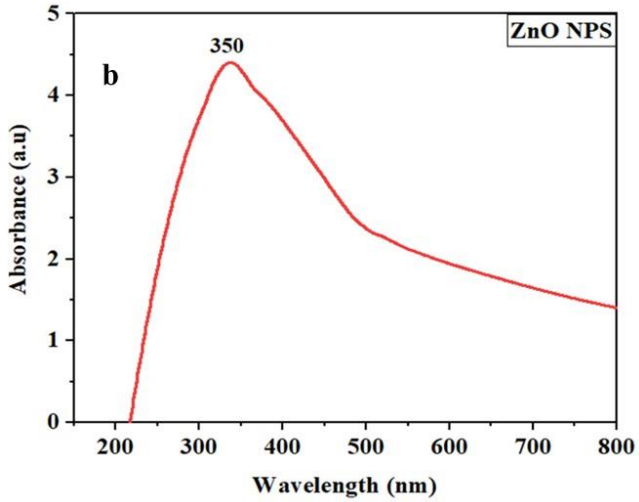


Figure 1. UV-Vis spectroscopy of the prepared nanoparticles

XRD displayed diffraction maxima near 32.5°, 34.1°, 37.5°, 48.1°, 56.3°, 63.5° and 67.2° (Figure 2). These reflections were indexed to the hexagonal ZnO lattice and were consistent with the reference pattern cited in the source manuscript. Application of the Scherrer equation yielded an average crystallite size of 68.3 nm. The result should be interpreted as crystallite size rather than an independent measurement of every particle visible by microscopy.

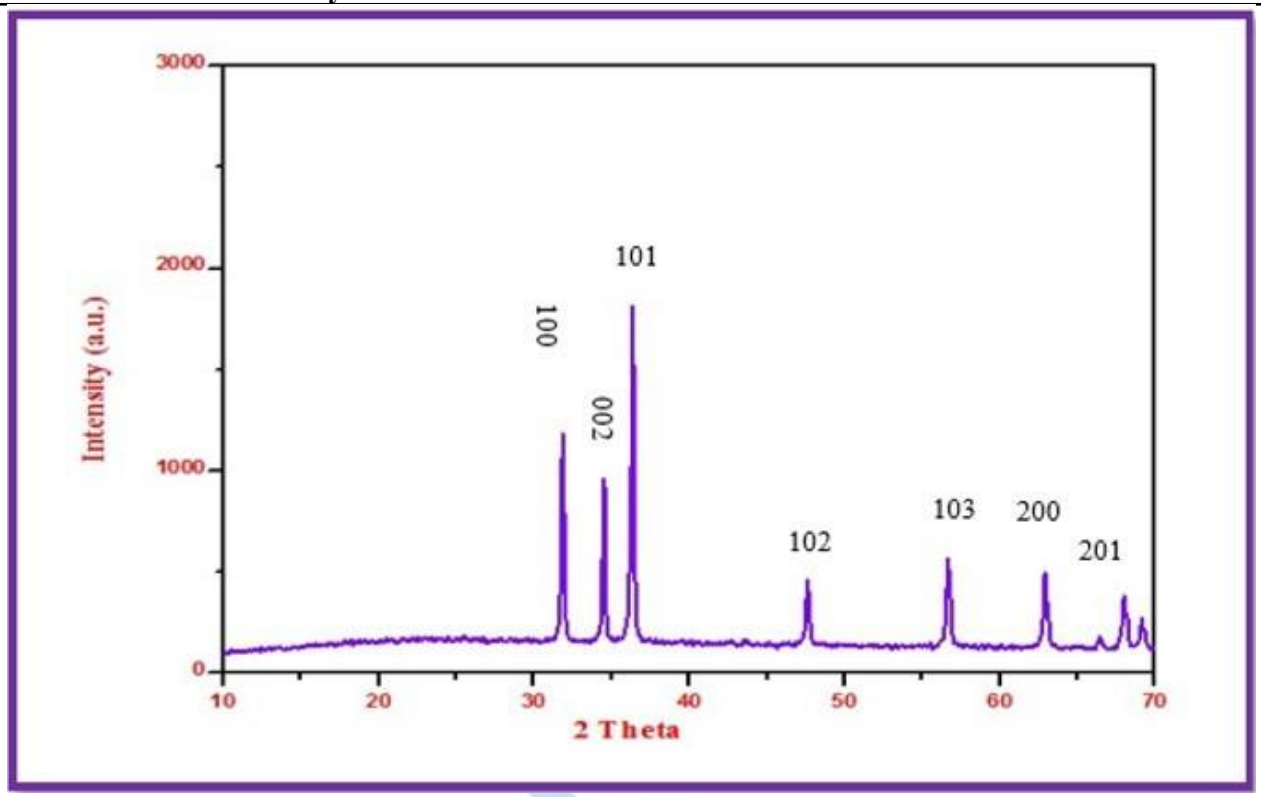


Figure 2. X-ray diffraction pattern of the synthesized ZnO nanoparticles.

FTIR spectra contained bands around 628.31, 833.52, 1222.51, 1417.10, 1609.90, 2167.65 and 3255.10 cm^{-1} (Figure 3). These bands indicate the presence of oxygen-, nitrogen-, and carbon-containing surface groups associated with organic residues from the plant extract. The spectrum therefore supports the participation of plant-derived molecules in surface modification, but FTIR alone does not establish the identity of individual phytochemicals.

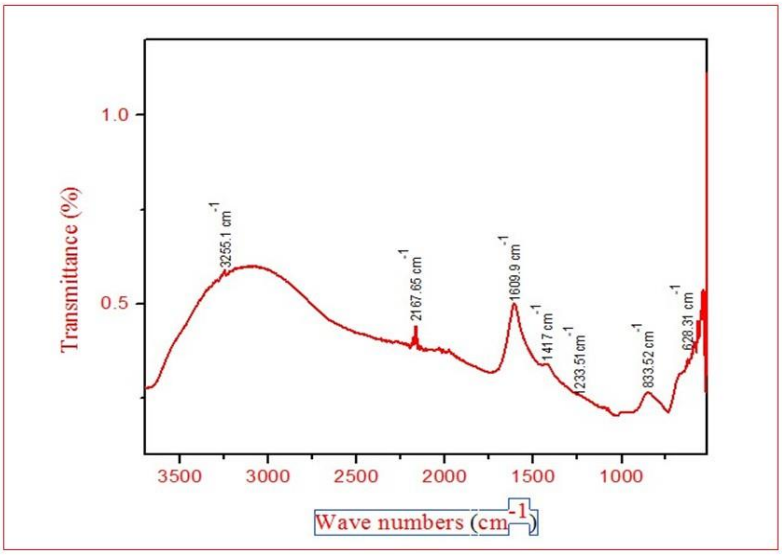


Figure 3. FTIR spectrum of the plant-mediated ZnO nanoparticles.

3.3 Morphology and elemental composition

SEM examination showed predominantly clover-leaf-like aggregates with a relatively homogeneous distribution in the observed field (Figure 4a). The morphology is consistent with the formation of irregularly assembled nanoscale structures. EDX confirmed zinc and oxygen as the principal inorganic elements, while carbon and sodium were also detected. The reported weight percentages were 51.4% Zn, 20.8% O, 20.8% C, and 6.9% Na; carbon and sodium may reflect residual plant-derived or processing-related components (Figure 4b).

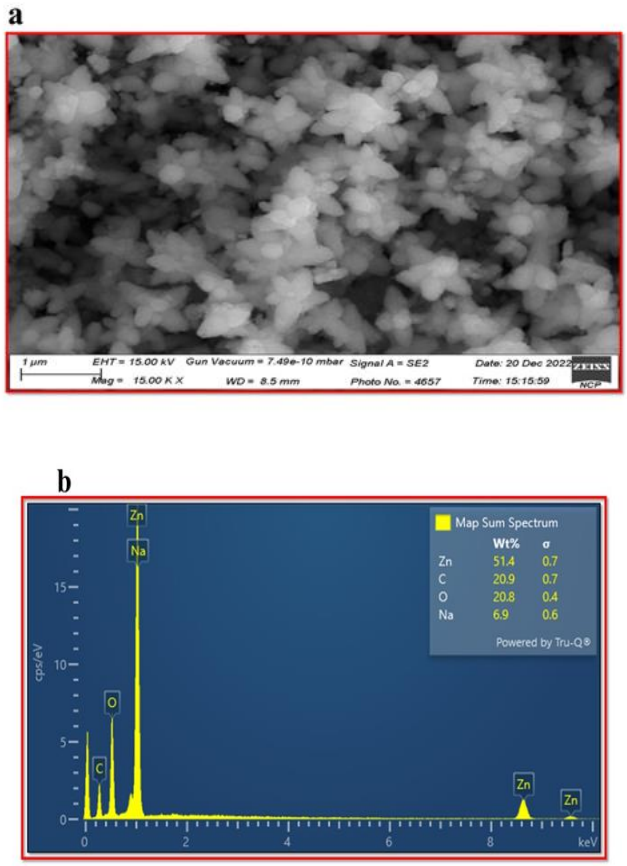


Figure 4. SEM morphology (a) and EDX spectrum (b) of the synthesized ZnO nanoparticles.

3.4 Surface charge and hydrodynamic size

The measured zeta potential was −8.95 mV, indicating a negatively charged nanoparticle surface under the tested dispersion conditions. DLS gave a zeta-average hydrodynamic diameter of 663.5 nm and a PDI of 0.523. The much larger hydrodynamic diameter than the XRD crystallite size suggests aggregation or clustered behavior in suspension, emphasizing the difference between crystallite dimensions and dispersed-particle hydrodynamic dimensions. All these results are depicted in Figure 5.

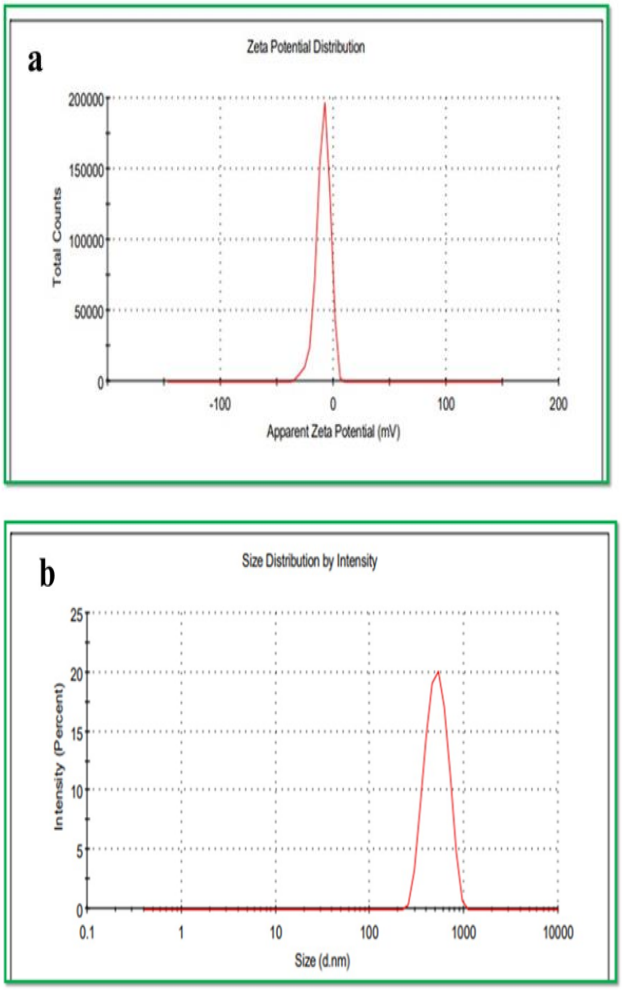


Figure 5. Zeta-potential profile and DLS intensity distribution of the ZnO nanoparticles.

3.5 Antileishmanial activity

The nanoparticles showed concentration- and time-dependent inhibition of L. tropica promastigotes. At 24 h, inhibition was 20, 30, 32 and 37% at 20, 40, 80 and 160 μg mL^{-1}, respectively (Figure 6). At 48 h, the corresponding values were 27, 32, 39 and 48%. At 72 h, inhibition increased to 35, 48, 60 and 68%, respectively. The supplied dataset therefore indicates the strongest response at 160 μg mL−1 after 72 h. ZnO-associated oxidative stress, surface interaction and zinc-ion release have been proposed as possible contributors to antiparasitic effects in related studies, but the present experiment did not directly distinguish among these mechanisms.

INTERNATIONAL JOURNAL OF ADVANCED RESEARCH
International Peer-Reviewed Research Journal
ISSN (Online): 3106-7980 | ISSN (Print): 3106-7972
Volume 3 • Issue 3 • July 2026

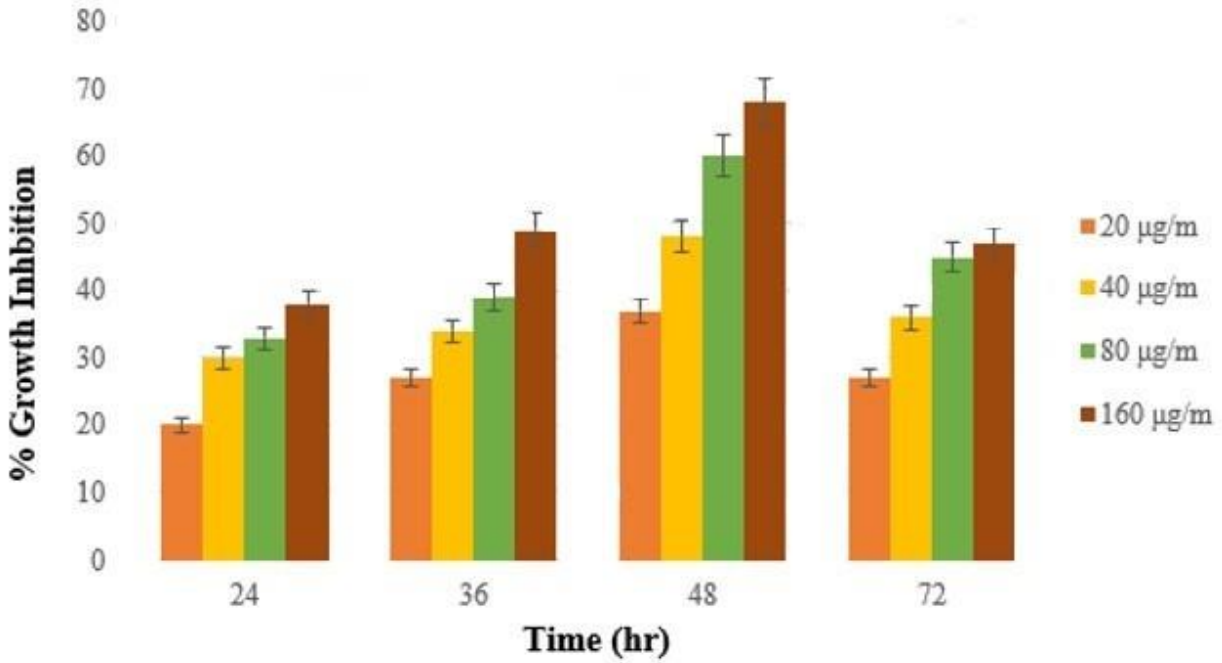


Figure 6. Antileishmanial response of ZnO nanoparticles at different concentrations and exposure times.

3.6 Pharmacological activity: protein denaturation inhibition

ZnO-NPs inhibited heat-induced BSA denaturation in a concentration-dependent manner. The recorded inhibition values were 45% at 50 µg mL^{-1}, 58% at 100 µg mL−1, 65% at 200 µg mL^{-1}, 70% at 400 µg mL^{-1} and 78% at 800 µg mL^{-1} (Figure 7). The assay provides an in vitro indication of anti-inflammatory potential, but it should not be interpreted as evidence of clinical anti-inflammatory efficacy.

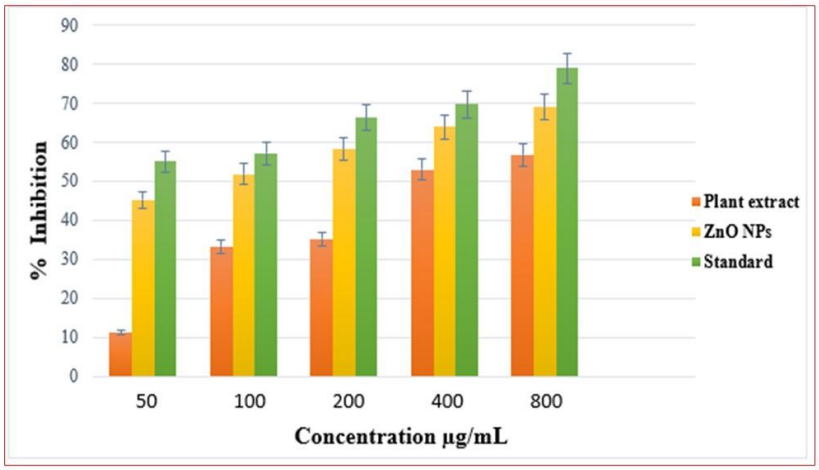


Figure 7. In-vitro inhibition of protein denaturation by ZnO nanoparticles.

3.7 Antioxidant responses

The antioxidant screening showed measurable activity across the tested assays. TAC reached 79.1% at 200 µg mL^{-1}, while TRP reached 65.2% at the same concentration. DPPH radical-scavenging activity reached 68.7% at the

highest concentration reported in the source dataset. These responses may reflect surface-associated plant-derived compounds and/or the redox-active behavior of the nanoparticle system; mechanistic attribution would require additional chemical analysis.

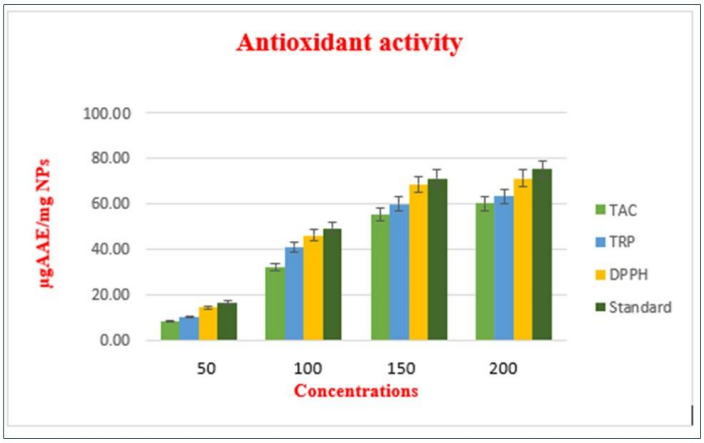


Figure 8. Total antioxidant capacity, reducing power and DPPH radical-scavenging responses.

International Journal of Advanced Research

3.8 Antimicrobial activity

Against E. *coli*, inhibition zones increased from 10.2 mm at 5 mg mL^{-1} to 17.4 mm at 10 mg mL^{-1} and 22.1 mm at 20 mg mL^{-1}. The concentration-dependent pattern indicates measurable antibacterial activity under the assay conditions. ZnO-mediated microbial inhibition has been associated in the literature with nanoparticle attachment, membrane perturbation, reactive oxygen species, and zinc-ion effects. These mechanisms remain plausible explanations rather than experimentally separated mechanisms in the present work.

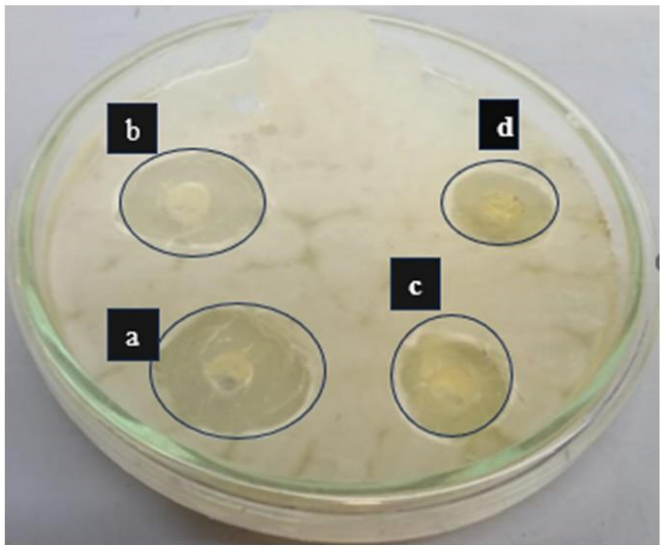


Figure 9. Antibacterial inhibition of *E. coli* by ZnO nanoparticles.

The antifungal assay against A. rabiei showed 56.77 ± 0.5% inhibition at 0.50 mg mL^{-1}, 66 ± 1.7% at 0.75 mg mL^{-1}, and 85 ± 2.1% at 1.0 mg mL^{-1} (Figure 10). The increasing response suggests that nanoparticle concentration was an important determinant of fungal growth suppression. Aggregation at higher doses may alter effective surface area and could explain deviations from a simple linear concentration-response relationship.

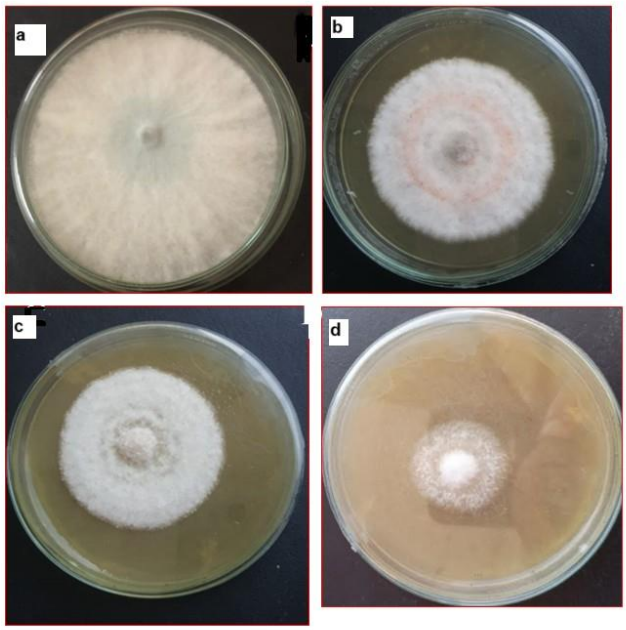


Figure 10. Antifungal activity of ZnO nanoparticles against Ascochyta rabiei.

3.9 Cadmium adsorption and environmental application

3.9.1 Effect of contact time

Cadmium uptake increased during the 5–120 min contact period, with the highest reported adsorption capacity reaching 85.3 mg g−1 at 120 min (Figure 11). The rapid initial stage can be attributed to the availability of unoccupied surface sites, followed by a slower approach toward equilibrium as those sites become progressively occupied. This behavior is characteristic of many adsorption systems and is consistent with the high surface-area rationale for nanoparticle-based remediation.

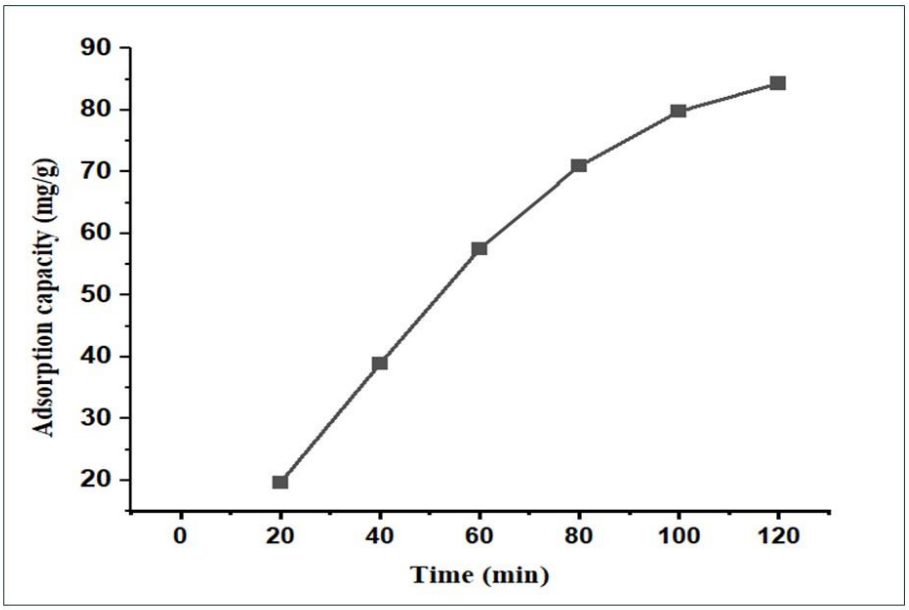


Figure 11. Effect of contact time on cadmium adsorption by ZnO nanoparticles.

3.9.2 Adsorption kinetics

The adsorption data were evaluated using pseudo-first-order and pseudo-second-order kinetic models. The supplied analysis reported a stronger fit for the pseudo-second-order model, suggesting that the empirical kinetics were better represented by this model under the tested conditions (Figre 12). This statistical fit should not, by itself, be treated as definitive proof of a particular molecular adsorption mechanism.

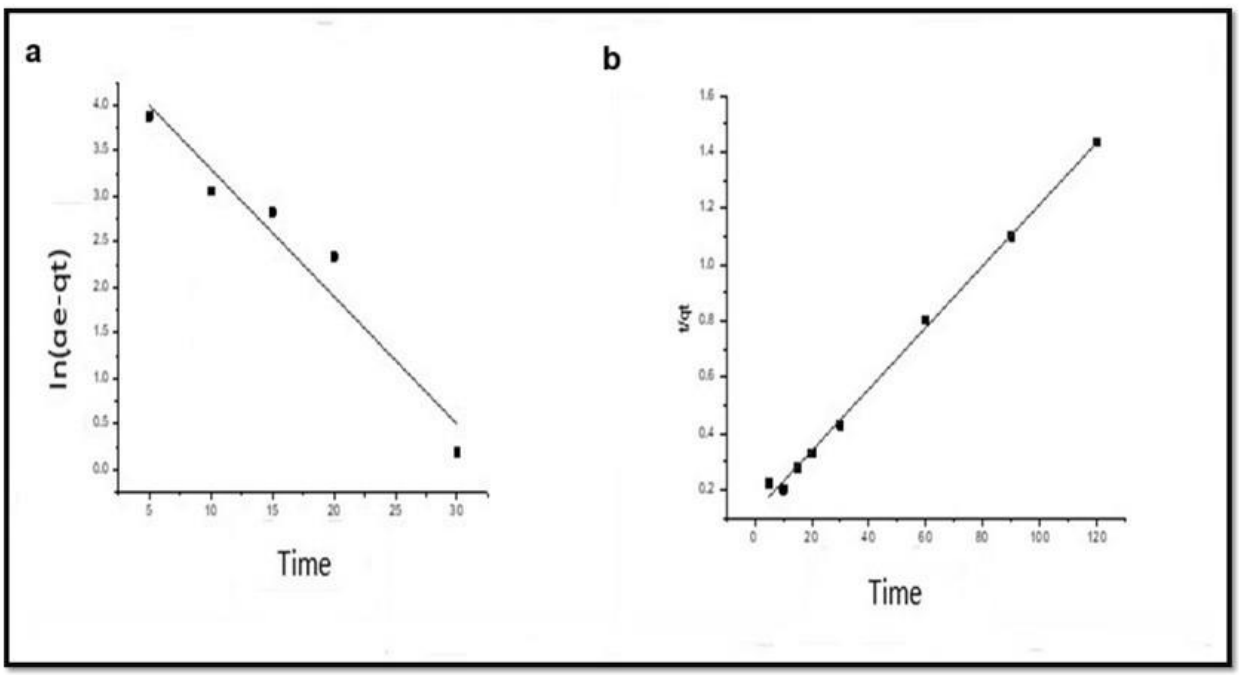


Figure 12. Kinetic-model analysis of cadmium adsorption.

3.9.3 Effect of initial Cd concentration

Increasing the initial Cd concentration from 20 to 120 mg L^{-1} increased the measured adsorption capacity, with 80.3 mg g^{-1} reported at 120 mg L^{-1}. The higher loading can be associated with a greater concentration gradient and increased probability of Cd interaction with available adsorption sites. At sufficiently high loading, however, progressive occupation of active sites is expected to limit further uptake.

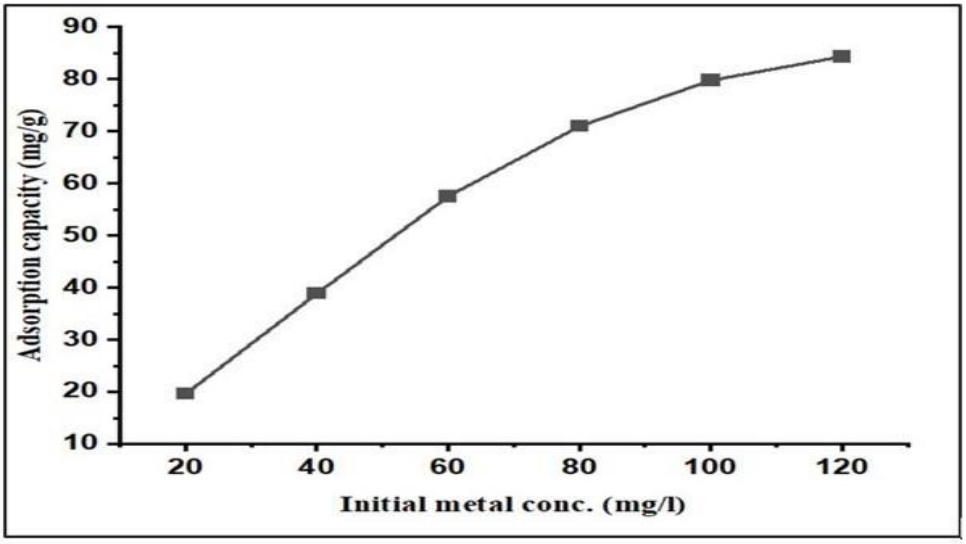


Figure 13. Influence of initial cadmium concentration on ZnO-NP adsorption performance.

3.9.4 Adsorption isotherms

Langmuir and Freundlich models were used to interpret equilibrium adsorption. The source dataset reported a stronger Langmuir fit and a maximum Langmuir adsorption capacity of 85.6898 mg g^{-1} (Figure 14). The reported Freundlich 1/n value was 0.3013, indicating favorable adsorption within the model framework. These findings support the usefulness of the synthesized material as an adsorbent under the studied laboratory conditions.

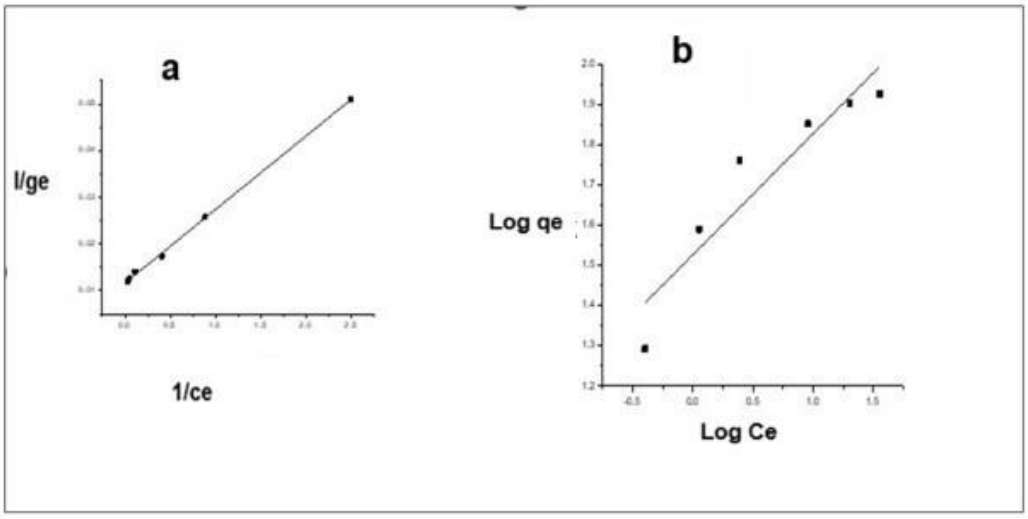


Figure 14. Langmuir and Freundlich isotherm plots for cadmium adsorption.

4. Discussion

The present study demonstrates the successful preparation of ZnO nanoparticles through a plant-mediated approach using *Ziziphus nummularia* leaf extract and highlights their potential for antimicrobial, pharmacological, environmental, and prospective photocatalytic applications. Plant-assisted synthesis has attracted considerable attention because phytochemicals present in plant extracts can participate in nanoparticle formation and stabilization while reducing the dependence on harsh chemical reagents. Phenolic compounds, flavonoids, terpenoids, proteins and other functional constituents can interact with zinc precursors and influence nucleation, growth and surface functionalization of ZnO nanoparticles (Basnet et al., 2018; Singh et al., 2016). Such biological surface modification may also influence the subsequent physicochemical and biological behavior of the nanoparticles.

The characterization results provide evidence for the formation of crystalline ZnO nanoparticles. The XRD analysis produced a calculated crystallite size of 68.3 nm, while the optical analysis indicated a band-gap value of 2.71 eV. The difference between crystallite size and hydrodynamic particle size observed in the present study is expected because these parameters describe different structural characteristics. XRD estimates the coherent crystalline domain, whereas DLS measures the hydrodynamic diameter of dispersed particles and aggregates. ZnO is a semiconductor whose optical and surface properties are strongly influenced by crystallinity, morphology, particle size, defects and surface chemistry. These characteristics are important because they can determine the antimicrobial, adsorption and photocatalytic performance of ZnO nanoparticles (Theerthagiri et al., 2019; Raha and Ahmaruzzaman, 2022). The DLS results showed a hydrodynamic diameter of 663.5 nm and a polydispersity index of 0.523. The considerably larger hydrodynamic diameter compared with the XRD crystallite size suggests that aggregation occurred in the dispersion used for DLS measurement. Such differences are frequently observed in nanoparticle systems because individual crystalline domains can associate into larger clusters in aqueous media. The measured zeta potential of −8.95 mV indicates a negatively charged particle surface under the experimental conditions. The relatively low magnitude of the zeta potential may partly explain the aggregation behavior observed by DLS. Particle aggregation and surface charge are important considerations because they can modify nanoparticle–microorganism interactions, adsorption behavior, and colloidal stability.

The FTIR and EDX results further support the formation and surface functionalization of the synthesized ZnO nanoparticles. Plant-mediated synthesis can leave phytochemical residues or functional groups on nanoparticle surfaces, which may contribute to stabilization and influence subsequent biological interactions. Previous research has demonstrated that plant-derived ZnO nanoparticles can contain surface-associated organic functional groups originating from the biological extract used during synthesis (Basnet et al., 2018). In addition, EDX detection of zinc and oxygen is consistent with the elemental composition expected for ZnO. Similar characterization approaches have been widely employed to confirm the formation of biologically synthesized ZnO nanoparticles (Miri et al., 2019; El-Saadony et al., 2024).

The use of *Ziziphus nummularia* is particularly relevant because this plant has previously been investigated for the biological synthesis of ZnO nanoparticles. Padalia and Chanda (2017) synthesized ZnO nanoparticles using *Z. nummularia* leaf extract and reported spherical to irregular particles with a mean size of approximately 17.33 nm. Their nanoparticles demonstrated considerable antifungal activity and cytotoxic effects against HeLa cells, supporting the potential of *Z. nummularia* as a useful biological source for ZnO nanoparticle production. The differences between their reported particle size and the present XRD/DLS measurements may reflect differences in synthesis conditions, calcination, extract composition and characterization methods rather than a contradiction between the studies.

The antimicrobial results obtained in the present study showed a concentration-dependent response against *Escherichia coli*. The

inhibition zone increased from 10.2 mm at 5 mg mL−1 to 22.1 mm at 20 mg mL−1, indicating progressively greater bacterial inhibition with increasing nanoparticle concentration. Similar concentration-dependent antibacterial activity has been widely reported for plant-mediated ZnO nanoparticles. ZnO nanoparticles may interact directly with microbial cell surfaces, disturb membrane integrity, promote reactive oxygen species generation, and release Zn^{2+} ions, all of which can contribute to microbial inhibition (Sirelkhatim et al., 2015; Tiwari et al., 2018). The relative contribution of each mechanism depends on particle size, morphology, surface charge, concentration and environmental conditions. Recent studies also indicate that phytochemicals associated with plant-mediated ZnO nanoparticles can modify their surface characteristics and antimicrobial activity (Sohrabi et al., 2026). The antifungal assay against *Ascochyta rabiei* showed a similar concentration-dependent pattern, with inhibition increasing from 56.77 ± 0.5% at 0.50 mg mL−1 to 85 ± 2.1% at 1.0 mg mL−1. This observation is consistent with previous reports demonstrating antifungal properties of ZnO nanoparticles. Importantly, the study of Padalia and Chanda (2017) using *Z. nummularia*-mediated ZnO nanoparticles reported strong antifungal activity against multidrug-resistant clinical isolates. Their findings provide particularly relevant support for the antifungal potential of the plant-mediated material investigated in the present study.

The observed antimicrobial effects can plausibly be associated with multiple nanoparticle-mediated mechanisms. ZnO nanoparticles may generate reactive oxygen species at the particle–cell interface, causing oxidative damage to cellular components. Zn^{2+} release can additionally disturb cellular metabolism, while direct physical contact with the microbial membrane can increase membrane permeability and cause structural damage. However, the present study did not independently quantify ROS production, Zn^{2+} release or membrane damage. Therefore, these mechanisms should be considered possible explanations based on established ZnO nanoparticle literature rather than experimentally demonstrated mechanisms in the present work. Reviews of plant-mediated ZnO nanoparticles similarly identify ROS generation, zinc-ion release and direct nanoparticle–cell interactions among the principal proposed antimicrobial mechanisms (Siddiqi and Husen, 2018; Tiwari et al., 2018). The pharmacological screening further demonstrated several biological responses. In the heat-induced BSA denaturation assay, inhibition increased from approximately 45% at 50 µg mL−1 to 78% at 800 µg mL−1. This concentration-dependent inhibition indicates that the ZnO nanoparticle preparation interfered with protein denaturation under the experimental conditions. Protein-denaturation assays are commonly used as preliminary in vitro screening approaches for anti-inflammatory activity. Nevertheless, this assay does not directly demonstrate anti-inflammatory efficacy in a biological system. Accordingly, the present findings should be interpreted as evidence of an in vitro pharmacological response requiring confirmation using cellular and in vivo models. Plant-mediated ZnO nanoparticles have previously been investigated for antioxidant, anti-inflammatory, anticancer, and other biomedical activities (El-Saadony et al., 2024; Siddiqi and Husen, 2018).

The antioxidant assays also demonstrated appreciable activity. Total antioxidant capacity reached 79.1%, reducing power reached 65.2%, and DPPH radical-scavenging activity reached 68.7% under the reported experimental conditions. The antioxidant response may be influenced by both the ZnO nanoparticle surface and phytochemicals originating from *Z. nummularia*. Phenolic and flavonoid compounds present in plant extracts can act as electron or hydrogen donors, while nanoparticle surface properties can additionally affect interactions with reactive species. Consequently, it would be inappropriate to attribute the entire antioxidant effect exclusively to ZnO without experiments separating the contribution of the plant extract from that of the nanoparticle. Previous reviews have emphasized the antioxidant potential of plant-mediated ZnO nanoparticles and the

importance of phytochemical capping layers in determining biological activity (El-Saadony et al., 2024; Abdel-Rahman et al., 2022). The antileishmanial assay showed increasing inhibition with both nanoparticle concentration and exposure time, reaching 68% inhibition at 160 μg mL−1 after 72 h. This finding indicates that the synthesized ZnO nanoparticles exerted measurable inhibitory activity against *Leishmania tropica* under the tested conditions. ZnO-based nanomaterials have previously been investigated for antiparasitic and biomedical applications, and their biological activity has been associated with oxidative stress, nanoparticle–cell interactions, and zinc-ion-mediated cellular effects. However, because ROS production, intracellular zinc accumulation, and parasite-specific molecular damage were not measured in the present study, the precise mechanism responsible for the observed antileishmanial activity remains unresolved.

The cadmium-removal experiment demonstrated significant adsorption capacity, with Cd uptake increasing with contact time and reaching 85.3 mg g−1 at 120 min. The rapid initial uptake followed by a slower phase can be interpreted as rapid occupation of readily accessible surface sites followed by progressive saturation of the remaining sites. Nanostructured ZnO possesses surface functional groups and a large interfacial area that can facilitate interaction with dissolved metal ions. The adsorption behavior of ZnO-based nanomaterials depends on surface charge, pH, particle aggregation, available binding sites and the chemical form of the target metal. Such properties make ZnO-based materials relevant to environmental remediation studies (Theerthagiri et al., 2019; Raha and Ahmaruzzaman, 2022). The kinetic analysis indicated a better fit to the pseudo-second-order model. This mathematical behavior suggests that the adsorption data were more appropriately represented by the pseudo-second-order equation than by the alternative kinetic model examined. Nevertheless, kinetic-model fitting alone should not be used to establish a particular molecular adsorption mechanism. Surface complexation, electrostatic attraction and interaction with oxygen-containing functional groups may occur simultaneously. Spectroscopic examination of the nanoparticle surface before and after Cd adsorption would be necessary to determine the specific surface groups involved. The equilibrium experiment showed an increase in adsorption capacity with increasing initial Cd concentration, reaching a reported maximum of 80.3 mg g−1 at 120 mg L−1. Increasing the initial concentration increases the concentration gradient between the solution and adsorbent surface and can therefore enhance mass transfer toward available adsorption sites. The reported Langmuir maximum adsorption capacity of 85.6898 mg g−1 and the stronger Langmuir model fit indicate that the Langmuir equation provided the better empirical representation of the equilibrium data. The calculated Freundlich 1/n value of 0.3013 also indicates favorable adsorption within the assumptions of the Freundlich model. Nevertheless, further experiments using real wastewater matrices, competing ions and regeneration cycles would be required before practical environmental application can be evaluated.

The photocatalytic potential of the synthesized ZnO nanoparticles is supported by their semiconductor properties and by the extensive literature on plant-mediated ZnO photocatalysts. ZnO can generate electron–hole pairs under suitable irradiation, and the resulting reactive species can participate in the transformation of adsorbed organic pollutants. Plant-mediated ZnO nanoparticles have been investigated for photocatalytic degradation of dyes and other contaminants, with particle size, morphology, band gap, surface defects and phytochemical functionalization influencing photocatalytic efficiency (Basnet et al., 2018; Fagier, 2021). Recent reviews have also emphasized that plant-mediated ZnO nanoparticles have potential for both antibacterial and photocatalytic applications and that synthesis conditions strongly influence these properties. However, the present Cd-removal experiment should not itself be described as photocatalytic degradation because the reported experiment evaluated adsorption rather than light-driven degradation. Demonstration of photocatalytic application

would require a dedicated experiment involving a defined light source, pollutant concentration, irradiation time, dark adsorption control, photolysis control and degradation kinetics. Therefore, photocatalysis should presently be discussed as a potential application of the synthesized ZnO nanoparticles rather than as an experimentally demonstrated property. This distinction is important because ZnO photocatalytic activity is strongly dependent on illumination conditions and material characteristics (Fagier, 2021; Mutukwa et al., 2024).Overall, the findings indicate that *Ziziphus nummularia*-mediated ZnO nanoparticles possess a combination of physicochemical, antimicrobial, pharmacological, and adsorption-related properties.

4. Conclusion

The revised manuscript presents a plant-mediated route for the preparation of ZnO nanoparticles using Ziziphus nummularia leaf extract and consolidates their physicochemical, antimicrobial, pharmacological, and environmental characteristics. The retained dataset indicates a 68.3 nm crystallite size, 2.71 eV optical band gap, −8.95 mV zeta potential and 663.5 nm hydrodynamic diameter. The nanoparticles showed concentration-dependent antileishmanial, anti-inflammatory, antibacterial, and antifungal responses, together with measurable antioxidant capacity. Cadmium adsorption reached 85.3 mg g^{-1} at 120 min, and the Langmuir model provided the stronger equilibrium fit in the supplied analysis. The material therefore demonstrates multifunctional laboratory-scale performance. Because the botanical identity was changed from the source manuscript to Z. nummularia, the plant authentication and all plant-dependent experimental observations should be verified against the actual material and voucher before submission. Likewise, photocatalytic application should be supported by a dedicated irradiation-based experiment rather than inferred from adsorption data.

Ethics approval and consent for publication: Not applicable

Consent for publication: Not applicable

Availability of data and material: The datasets generated and/or analysed during the current study are not publicly available due to confidentiality and ongoing research use (as the data form part of continuing research work and institutional records), but are available from the corresponding author on reasonable request.

Competing interests: All the authors in the article have declared that there is no conflict of interest among them.

Funding: Not applicable

Author Contributions

Muhammad Rashid Naveed: Conceptualization, Methodology, Investigation, Data curation, and Writing – original draft. Sehrish Javed: Investigation, Data curation, Formal analysis, and Visualization. Rizwan Ullah: Conceptualization, Methodology, Supervision, Project administration, and Writing – review & editing. Mumtali Shah: Investigation, Formal analysis, and Validation. Rabail Urooj: Data curation, Visualization, and Writing – review & editing. Binyamin Siddiqui: Resources, Validation, and Writing – review & editing. Rahman Ullah Khan: Supervision, Funding acquisition, Project administration, and Writing – review & editing. All authors reviewed and approved the final version of the manuscript.

Acknowledgments: We are thankful to all the researchers who contributed to the research work.

REFERENCES

Ali, J., Irshad, R., Li, B., Tahir, K., Ahmad, A., Shakeel, M., et al. (2018). Synthesis and characterization of phytochemical fabricated zinc oxide nanoparticles with enhanced antibacterial and catalytic applications. *Journal of Photochemistry and Photobiology B: Biology, 183*, 349–356.

Arora, A. K., Devi, S., Jaswal, V. S., Singh, J., Kinger, M., & Gupta, V. D. (2014). Synthesis and characterization of ZnO nanoparticles. *Oriental Journal of Chemistry, 30*(4), 1671–1679.

Bhilkar, P. R., Bodhne, A. S., Yerpude, S. T., Madankar, R. S., Somkuwar, S. R., Daddemal-Chaudhary, A. R., Lambat, A. P., Desimone, M., Sharma, R., & Chaudhary, R. G. (2023). Phyto-derived metal nanoparticles: Prominent tool for biomedical applications. *OpenNano, 14*, 100192. SciELO

Dadi, R., Azouani, R., Traore, M., Mielcarek, C., & Kanaev, A. (2019). Antibacterial activity of ZnO and CuO nanoparticles against Gram-positive and Gram-negative strains. *Materials Science and Engineering: C, 104*, 109968.

El-Belely, E. F., Farag, M. M. S., Said, H. A., et al. (2021). Green synthesis of zinc oxide nanoparticles and evaluation of their biomedical activities. *Nanomaterials*.

Eleryan, A., et al. (2023). Reference concerning nanostructured adsorbents and heavy-metal removal. Full bibliographic details should be checked against the original reference source before submission.

Emami-Karvani, Z., & Chehrazi, P. (2011). Antibacterial activity of ZnO nanoparticle on Gram-positive and Gram-negative bacteria. *African Journal of Microbiology Research*.

Fagier, M. A. (2021). Plant-mediated biosynthesis and photocatalysis activities of zinc oxide nanoparticles: A prospect towards dyes mineralization. *Journal of Nanotechnology*.

Janaki, A. C., Sailatha, E., & Gunasekaran, S. (2015). Synthesis, characteristics and antimicrobial activity of ZnO nanoparticles. *Spectrochimica Acta Part A: Molecular and Biomolecular Spectroscopy, 144*, 17–22.

Kaewsarn, P. (2002). Low-cost biosorbent for heavy-metal removal from aqueous solution. *Bioresource Technology*.

Kaushik, M., Niranjan, R., Thangam, R., Madhan, B., Pandiyarasan, V., Ramachandran, C., et al. (2019). Investigations on the antimicrobial activity and wound-healing potential of ZnO nanoparticles. *Applied Surface Science, 479*, 1169–1177.

Khalafi, T., Buazar, F., & Ghanemi, K. (2019). Phycosynthesis and enhanced photocatalytic activity of zinc oxide nanoparticles toward organosulfur pollutants. *Scientific Reports, 9*, 6866. Nature

Khan, M., et al. (2023). Reference concerning pharmacological/biological activity of green-synthesized ZnO nanoparticles. Full details should be verified from the original reference list.

Modi, S., et al. (2023). Reference concerning antimicrobial mechanisms/properties of ZnO nanoparticles. Full bibliographic details should be verified.

Moavi, J., Buazar, F., & Sayahi, M. H. (2021). Algal magnetic nickel oxide nanocatalyst in accelerated synthesis of pyridopyrimidine derivatives. *Scientific Reports, 11*, 6296. Nature

Muhammad, et al. (2019). Reference used for the heat-induced BSA denaturation/anti-inflammatory assay. Full bibliographic details should be verified from the original manuscript reference list.

Nazir, S., Rabbani, A., Mehmood, K., Maqbool, F., Shah, G. M., Khan, M. F., & Sajid, M. (2019). Antileishmanial activity and cytotoxicity of ZnO-based nano-formulations. *International Journal of Nanomedicine, 14*, 7809–7822.

Onyancha, D., et al. (2022). Reference concerning nanostructured adsorbents and heavy-metal removal. Full bibliographic details should be verified.

Pantidos, N., & Horsfall, L. E. (2014). Biological synthesis of metallic nanoparticles by bacteria, fungi and plants. *Journal of Nanomedicine & Nanotechnology, 5*.

Padalia, H., & Chanda, S. (2017). Characterization, antifungal and cytotoxic evaluation of green synthesized zinc oxide nanoparticles using *Ziziphus nummularia* leaf extract. *Artificial Cells, Nanomedicine, and Biotechnology, 45*(8), 1751–1761. https://doi.org/10.1080/21691401.2017.1282868.

Perwez, M., Lau, S. Y., Hussain, D., Anboo, S., Arshad, M., & Thakur, P. (2023). Nanozymes and nanoflower: Physiochemical properties, mechanism and biomedical applications. *Colloids and Surfaces B: Biointerfaces, 225*, 113241.

Raha, S., & Ahmaruzzaman, M. (2022). ZnO nanostructured materials and their potential applications: Progress, challenges and perspectives. *Nanoscale Advances, 4*, 1868–1925.

Siddiqi, K. S., & Husen, A. (2016). Fabrication of metal and metal oxide nanoparticles by algae and their toxic effects. *Nanoscale Research Letters, 11*, 363.

Siddique Afridi, et al. (2018). Reference used for the *Leishmania tropica* experimental methodology. Full bibliographic details should be verified against the original reference source.

Siripireddy, B., & Mandal, S. (2017). Reference concerning ZnO photocatalytic properties. Full bibliographic details should be verified before submission.

Theerthagiri, J., Salla, S., Senthil, R. A., Nithyadharseni, P., Madhankumar, A., Arunachalam, P., et al. (2019). A review on ZnO nanostructured materials: Energy, environmental and biological applications. *Nanotechnology, 30*, 392001.

Tiwari, V., Mishra, N., Gadani, K., Solanki, P. S., Shah, N. A., & Tiwari, M. (2018). Mechanism of anti-bacterial activity of zinc oxide nanoparticle against carbapenem-resistant *Acinetobacter baumannii*. *Frontiers in Microbiology, 9*, 1218.

Wang, X., et al. (2023). Reference concerning phytochemical/plant-mediated ZnO nanoparticle synthesis. The exact article should be verified. There are multiple Wang et al. (2023) papers on plant-mediated ZnO nanoparticles, so I would not assign a bibliographic record without checking the original source. For example, Wang et al. published a 2023 review on ZnO nanoparticle synthesis and plant stress applications.

Sharmila, G., Thirumarimurugan, M., & Muthukumaran, C. (2019). Green synthesis of ZnO nanoparticles using *Tecoma castanifolia* leaf extract: Characterization and evaluation of its antioxidant, bactericidal and anticancer activities. *Microchemical Journal, 145*, 578–587.

Sarkar, et al. (2014). Reference used for nanoparticle/DLS characterization. Full bibliographic information should be verified from the source manuscript.

Ho, Y. S., & McKay, G. (1998). Kinetic models for the sorption of dye from aqueous solution by wood. *Process Biochemistry, 34*, 451–465.

Al Rugaie, O., et al. (2022). Reference concerning ZnO nanoparticle antimicrobial activity. Full bibliographic details should be verified from the original reference list.

Aldeen, T. S., Mohamed, H. E. A., & Maaza, M. (2022). ZnO nanoparticles prepared via a green synthesis approach: Physical properties, photocatalytic and antibacterial activity. *Journal of Physics and Chemistry of Solids, 160*, 110313.